

DISK MASS ESTIMATES IN A BINARY SYSTEM

E. Nagel

Instituto de Astronomía
Universidad Nacional Autónoma de México, Mexico

Received 2007 April 30; accepted 2007 November 21

RESUMEN

Desde el punto de vista analítico, un asunto natural de estudio en un sistema binario en órbita circular es la consecuencia de la conservación de la constante de Jacobi (C_J). La implicación principal es que para cada partícula existen zonas permitidas y prohibidas. Este esquema es válido al incluir interacciones entre las partículas; esto únicamente significa que C_J y el espacio de configuración permitido-prohibido depende del tiempo. La formación y evolución inicial de un disco alrededor de una estrella aislada se interpreta de acuerdo con este marco. Extendemos este modelo para el caso en el cual se tiene una estrella secundaria pequeña. Las estimaciones observacionales de la razón entre las masas del disco circunprimario y circumbinario son congruentes con un conjunto de simulaciones SPH en el cual la razón entre la separación entre las estrellas y el radio del disco es el parámetro que cambia. Se usa GW Ori como ejemplo.

ABSTRACT

The consequences of the conservation of the Jacobi constant (C_J) are studied here analytically for a circular binary system. The main result is that for every particle there are prohibited and allowed zones. This scheme is valid with the inclusion of interactions between the particles in the orbital plane of the binary system; this means that C_J and the allowed-prohibited configuration space are time-dependent. The formation and initial evolution of a disk around an isolated star is interpreted according to this work. We extend this model for the case where there is a small secondary star and argue that observational estimates of the ratio between circumprimary and circumbinary disk masses are consistent with a set of SPH simulations in which the ratio between the separation of the stars and the disk radius is the parameter that varies. GW Ori is used as an example.

Key Words: accretion, accretion disks — binaries: general — circumstellar matter

1. INTRODUCTION

Specific values of disk masses clearly depend on the details of their formation, including the characteristics of the parent cloud, and also the interactions between the disk and the binary system, or any other external influence. Additionally, direct observations of disks require very high spatial resolution. This is a difficult task, and in fact for the same system, circumstellar or circumbinary disks have not been resolved yet by observations. On top of that, the estimation of disk masses is clearly model-dependent (see § 2).

Numerical simulations (Bate 2000) of binary system formation suggest that a continuous infall from the cloud feeds the system until it arrives at its final

stable configuration. During this time a disk forms and continually loses material to the star, resulting in angular momentum transport, which is necessary for the material to accrete. This argument suggests that the final disk, formed during a characteristic time $\Delta t \ll t_{\text{ff}}$ (where t_{ff} is the free fall time for the last section of the cloud that forms the binary system), and the double dense ring pattern disk described in Nagel (2007a) is the expected outcome.

We describe the formation of disks in the state when material is still falling from the cloud into the orbital plane; thus, the system is in the embedded stage. Only now are observational techniques available that allow a system deep inside its parental cloud to be seen. An example of such a system is

NGC 1333 IRAS 4 (Smith et al. 2000), which is resolved as a binary system with a common envelope around both components. Hence, the idea of cloud material falling towards a binary seems reasonable. One of the components is the binary itself; its elongated shape can be interpreted as a circumbinary disk (Smith et al. 2000). A circumbinary disk is present in the collapsing stage, consistent with the configuration we are describing in this paper. The infall-disk interface has been observed in methanol emission (Velusamy, Langer, & Goldsmith 2002); thus, present technology permits the study of this kind of object.

Following Nagel (2007a), it is possible to estimate disk masses by dividing the material that falls from the cloud during the time Δt in three parts. The inner part of the cloud, which corresponds to material with the smallest values of specific angular momentum, is absorbed by the star. An intermediate zone of the cloud is associated to an inner ring (see Nagel 2007a). However, the material in this ring arrives later in the evolution; thus, it is not considered here. In this work, we consider a slab of material that lands in the orbital plane at some time, and represents all the mass accreted during a time Δt . The external part of the cloud with larger values of specific angular momentum will feed the outer dense ring as described in Nagel (2007a). In this paper we try to convince the reader that most of this material settles in the circumbinary disk; the remaining material finds its way to a circumstellar disk. In this way, we can assign relative masses to the circumbinary and circumstellar disks; this is described in § 4.4. All these parts correspond to the different ranges in the specific angular momentum (γ) of the cloud. If the scheme of an isolated star is assumed, then the mass of the secondary star (M_s) is much less than the mass of the primary star (M_p).

This paper approximates the problem as three-body interactions (a falling particle and two stars) assuming $M_s \ll M_p$, in order to explore the consequences of the conservation of the Jacobi constant (C_J). All this leads us to configurations with allowed and prohibited regions, where the zero-velocity surfaces (Szebehely 1967; Murray & Dermott 1999) are the boundaries between these zones. Relevant configurations are the ones that restrict some of the material inside the orbit of the secondary to form a circumprimary disk, and outside of it, to form a circumbinary disk. Similar ideas are applied in general to a planetary system around a binary system (Szebehely 1980) looking for stability of planets and for

outer planetary systems by Szebehely & McKenzie (1981).

The material associated with the circumprimary disk will be shared between both circumstellar disks when the secondary star is present. Our assumption is that $M_s \ll M_p$ allows for the larger mass star to attract most of this material. In this sense, the amount of material associated with a circumstellar disk correlates with the mass of the star. In our analysis, we do not generate any estimation for the secondary disk mass; thus, we cannot determine how small it is compared with the other two disks.

The radii where the curves of zero-velocity are located in the orbital plane are given in units of the separation between the stars (a). The ratio between a and the other distance of the problem, R_d , is called $y = a/R_d$. Here, R_d is a typical disk size. y measures the importance of angular momentum transport processes during the binary system formation (see § 3.2). Finally, we present a set of simulations for various values of this parameter y .

Thus, the aim of this paper is to give an estimation for the circumprimary and the circumbinary disk masses. For a precise estimation for both masses, a model including the interactions between particles and between the particles and the stars will be necessary.

We have organized the paper as follows: § 2 gives a review of the difficulties and uncertainties for the disk mass estimations from the observational point of view. The next section (§ 3) characterizes the falling cloud, pointing out the processes of angular momentum transport required for the material to arrive at the star. In § 4 we give a description for the restrictions obtained from the conservation of C_J when the 3-body approximation is used. § 5 analyzes a series of simulations that confirm the idea that the influence of the secondary star is able to restrict the material to circumprimary and circumbinary disks. The next section (§ 6) contains the main conclusions.

2. OBSERVATIONAL ESTIMATES OF DISKS MASS

From the observational viewpoint, at present it is not possible to easily disentangle the mass contribution of each disk from the total flux that is detected. The first targets were isolated stars, where it is easier to separate the flux from the disk from that of the star with the use of a model for the disk (Osorio et al. 2003; D'Alessio, Calvet, & Hartmann 1997). Both the identification and characterization of a disk in isolated stars or in binary systems require a model for the disk. An estimation of the disk mass, for instance of a disk seen edge-on, which hides some of

the radiation of the star (Stapelfeldt et al. 1998, for HK Tau/c) requires the assumption of some characteristics of the disk, such as temperature and opacity of the material.

In many cases the disk is not resolved; thus the spectral energy distributions (SEDs) should be interpreted with a model for the disk (designating surface density, temperature, inner and outer radius, opacity, etc.), which have many free parameters to fix. Isolated star studies are highly successful (Osorio et al. 2003; D'Alessio et al. 1997). However, for the binary systems, the number of free parameters increases (there are more disks), and the uncertainty attached to them makes the estimates unreliable (Mathieu 1994).

Some observations, mainly from mm to radio (Jensen & Akeson 2003; Weintraub, Zuckerman, & Masson 1989; Guilloteau, Dutrey, & Simon 1999), resolve the disk and impose very strong restrictions on the spatial distribution of material, at least a minimum value for the size of this region (undetected material outside it could exist). However, an assumption about the optical characteristics of the disk material is still required. On the other hand, tracing all the disk material from the intensity observed can be done with the assumption that all the material is optically thin (Jensen, Koerner, & Mathieu 1996; Jensen & Akeson 2003 for HK Tau, DK Tau and UX Tau and Mathieu et al. 1995 for GW Ori), which is commonly used. Thus, a given value for the opacity is always required; in GW Ori (Mathieu et al. 1995), a typical error in this quantity implies a factor of 3 in the estimate of the disk mass. Another parameter to fix is the temperature. Mass estimates in Mathieu et al. (1995) vary by a factor of two when the temperature does the same.

In unresolved disks, a common model is an optically thick α -disk (α prescription for the viscosity, Shakura & Sunyaev 1973) for the adjustment of the SED. In the case of UY Aur (Close et al. 1998), a suitable α gives disk-mass accretion rates in the range $\dot{M} \approx 10^{-8}$ to $10^{-7} M_{\odot} \text{ yr}^{-1}$ and disk masses ranging from $M_d \approx 10^{-6} M_{\odot}$ to $10^{-5} M_{\odot}$, accounting for both circumstellar disks.

The simplest disk configuration in a binary system is a disk around the primary; a gap that contains the orbit of the secondary which mimics the clearing effect of the binary (see Artymowicz & Lubow 1994), and a circumbinary disk (Mathieu et al. 1995; Jensen & Mathieu 1997). This configuration corresponds to the $M_s = 0$ case (see § 4.3).

The binary system GW Ori is analyzed imposing this configuration in Mathieu et al. (1995), who

find $M_p \approx 2.5 M_{\odot}$ and $M_s \approx (0.3 - 1.3) M_{\odot}$. Thus, taking the lower limit for M_s , it is reasonable to assume that $M_s = 0$. Moreover, the eccentricity of the binary orbit can be taken as $\epsilon = 0$ ($\epsilon = 0.04 \pm 0.06$ is given in Mathieu, Adams, & Latham 1991). Both choices (circular orbit and no secondary star), allow the application of the conclusions in § 4.3 and § 4.4 to this system for the comparison between both disk-mass estimates.

From the observational point of view, an *ad hoc* system has not been found until now because there are no images for circumstellar or circumbinary disks in the same system. This information is required to get a better estimate for both disk-masses. In conclusion, the observational estimations of these masses are strongly model-dependent, as well as the comparison of these results and the analysis presented in this paper.

Binary systems with separations of only a fraction of an AU are also very useful for our purposes, because such a configuration allows to easily find circumbinary disks (Bate 2000; Mathieu et al. 1995). One such system is UZ Tau E, for which $\epsilon = 0.237 \pm 0.030$ (close to a circular orbit) and $q = M_s/M_p = 0.28 \pm 0.01$. Remember that $\epsilon = 0$ and $q \ll 1$ are necessary assumptions in the models presented in § 4.3 and § 4.4.

Another important assumption throughout this work is that the circumbinary disk and the binary orbit are coplanar. T Tau is a system extensively studied (Hogerheijde et al. 1997; Weintraub et al. 1989), for which the masses of the circumstellar and circumbinary disks are estimated. Unfortunately there is evidence that the binary orbit and disks are not in the same plane (Hogerheijde et al. 1997). For HK Tau (Duchene et al. 2000), a 1.3 mm flux is observed either around the secondary or around the primary, but the material in the latter is not detected in the optical or near-infrared. Thus, for this system, it is suggested that the disks are not coplanar. It should be remembered that material falling from a rigidly rotating cloud (see § 3.1) naturally defines a symmetry plane (orbital plane), where the stars and disks should lie.

Four spectroscopic binary systems ($a < 1$ AU) are studied in Jensen & Mathieu (1997); the system that can be described by the method presented here is V4046 Sgr, ($a = 0.04$ AU), which is circular. Depletion of emission in the near-infrared suggests the existence of a gap cleared by the binary. Jensen & Mathieu (1997) use the radii for the boundaries of the gap, $R_{\text{in}} = 0.4a$ and $R_{\text{out}} = 1.8a$, given in Artymowicz & Lubow 1994. The observed SED cannot

be reproduced by a disk with this size. They allow variations in R_{in} and R_{out} and the best fit requires $R_{\text{in}} = R_{\star}$ (R_{\star} is the star radius) and $R_{\text{out}} = 0.18 \text{ AU}$; thus, in their interpretation for this system, only a circumbinary disk is present. This does not contradict our conclusions or typical observations (Dutrey, Guilloteau, & Simon 1994), because circumbinary disks are always present, and they are at least an order of magnitude more massive than the circumstellar ones (Duvert et al. 1998).

3. MAIN STATEMENTS

3.1. Characterization of material that falls from the cloud

The next step is to characterize the material that falls from the cloud towards the stellar system; this material will ultimately form the disk. The matter begins its collapse far away from the stars. Assuming that the cloud is rigidly rotating, the solution of Ulrich (1976) can be used to describe the initial velocity and trajectory of each particle. The cloud can be taken as rigidly rotating because the magnetic field lines tend to enforce it (Mouschovias & Paleologou 1979). However, in this paper we ignore the influence of the magnetic field, since the magnetic pressure is not enough to halt the collapse.

For the initial condition, our assumption is that a particle only feels the gravitational force of the central object, and thus Ulrich's solution can be taken. A necessary condition to take this solution is that R_{d} (the largest Keplerian orbit that can be formed) is larger than a (distance between the stars in a binary system). Here, this assumption is always used. In Nagel (2007a) the velocity field and density on the orbital plane were deduced, and it was also shown that the radius (in units of R_{d}) where a particle first intersects the orbital plane is equal to the specific angular momentum in units of γ_{∞} , which is the maximum specific angular momentum on the orbital plane at the time of disk formation. As described in Nagel (2007a), the angular momentum completely determines the evolution of the particles in this plane. For a disk in an isolated star this is the model required. For a binary system, the angular momentum is not an integral of motion, thus, the description of this three body problem should be done using the Jacobi constant C_{J} , which is the only quantity that is conserved in the circular restricted 3-body model (two stars and a particle). Both here and in the two-body problem, the conservation of the angular momentum defines a prohibited region; thus, material should not be at the left of the minimum radius curve (see Nagel 2007a for details). In

conclusion, in both cases, a conservation argument puts restrictions on the space, specifying where the material can exist.

3.2. Importance of angular momentum transport processes

As stated before, it is of crucial importance to compare the two characteristic distances of the problem, R_{d} and a . The latter is a parameter that can be obtained directly from observations of a particular system. The disk radius (R_{d}) is observationally difficult to establish. It depends on the cloud, which must be related to a , because the binary system forms from its collapse. A way to relate the two quantities is to assume that the angular momentum of the binary system (Γ_{b}) is equal to the angular momentum contained in the inner region of a rigidly rotating cloud (Γ_{c}); their expressions are given by:

$$\Gamma_{\text{b}} = \sqrt{GM_{\star}^3 a} \frac{q}{(1+q)^2} \quad , \quad (1)$$

$$\Gamma_{\text{c}} = \frac{2}{5} M_{\star} R_{\text{c}}^2 \Omega_{\text{c}} \quad , \quad (2)$$

where Ω_{c} is the angular velocity of the cloud. The stellar mass M_{\star} is contained within a spherical radius R_{c} and the cloud density prior to collapse is assumed uniform. The use of another density profile for the cloud changes the result quantitatively. However, the main conclusion is the same. Here, q is the stellar mass ratio $M_{\text{s}}/M_{\text{p}}$. Using the following realistic values: $a = 40 \text{ AU}$, $\Omega_{\text{c}} = 3.13 \times 10^{-14} \text{ s}^{-1}$ (Jijina, Myers, & Adams 1999; Bate 2000) and $M_{\star} = 2 M_{\odot}$, we find $R_{\text{d}} = 0.4a$, thus $R_{\text{d}} < a$.

This result is in conflict with the requirement that the edge of the disk must lie outside the orbit of the star, in order to form a circumbinary disk. Thus, the processes that transport angular momentum outside of the cloud are extremely necessary. Some momentum can be located in circumstellar and circumbinary disks, but to form the latter it is clearly required that $R_{\text{d}} > a$ in the first place; thus, some mechanisms are still required to remove the angular momentum that remains.

A way to address this issue is to note that in the problem of a particle falling towards a two body system, the angular momentum is no longer constant, but a detailed study is still necessary to quantify the losses in such a case. These losses are calculated by Bate (2000), where the evolution of a proto-binary seeded at the center of a collapsing cloud is studied. For the final configuration (all the mass of the cloud has accreted) of the simulation of his test (1) (collapse of a rigidly rotating, constant density, cloud),

the angular momentum assigned to the binary system is $\Gamma_b = 1.469 \times 10^{50} \text{ kg cm}^2 \text{ s}^{-1}$, and for the cloud it is $\Gamma_c = 2.49 \times 10^{50} \text{ kg cm}^2 \text{ s}^{-1}$. The condition $\Gamma_c > \Gamma_b$ is necessary for the formation of a disk. In the Bate (2000) simulation some angular momentum is contained in a disk-like structure that forms during the simulation. If it is assumed that it rotates with a Keplerian velocity and lies between a radius equal to a and $2a$, (typical values extracted from the configuration plots of Bate (2000)), we find $\Gamma_{cb} = 1.003 \times 10^{50} \text{ kg cm}^2 \text{ s}^{-1}$ for the angular momentum associated to the circumbinary disk. The conservation of angular momentum, $\Gamma_b + \Gamma_{cb} = \Gamma_c$ is not satisfied. From these calculations it can be said that some of the angular momentum disappears from the disk-stars system, fulfilling this requirement for the real case.

Magnetic braking can be an extremely efficient mechanism for outward transfer of angular momentum (see model by Galli et al. 2006) in the collapse of an isothermal magnetized rotating cloud. In such a case, the angular momentum is completely removed from the central part of the cloud. Thus, neither a disk nor a companion star can be formed. Dissipation of the magnetic field is required for the formation of a disk (Shu et al. 2006), in order for the existence of a state with not too extreme magnetic braking. Thus, at least there is this mechanism, which allows the parameter $y = a/R_d$ to decrease to reasonable values.

3.3. Accretion of mass towards the star from a disk

During the collapse phase, a protobinary system evolves with already formed disks, as there is nothing to prevent it. The time (t_d) needed to transport a typical amount of mass through the disk to the star can be estimated using a typical value for the mass accretion rate ($\dot{M} \approx 5 \times 10^{-8} M_\odot \text{ yr}^{-1}$, Hartmann & Kenyon 1990) and for the mass of observed disks ($M_d \approx 2 \times 10^{-2} M_\odot$, Beckwith et al. 1990). With these values, we get $t_d \approx 4 \times 10^5 \text{ yr}$, which is of the same order as the free-fall time (t_{ff}).

Besides, the estimate of t_d takes into account mass transfer mechanisms that occur slowly and continuously. However, at this early stage gravitational instabilities are present (Bodenheimer & Laughlin 1995; Boss 1998; Nakamoto & Nakagawa 1994; Yorke & Bodenheimer 1999) which are responsible for intermittent periods of enhanced transfer. Both arguments indicate that a large amount of the mass that falls on the orbital plane is driven to the star at the end of the collapse.

The model developed in Nagel (2007a) shows that a circumstellar disk contains a section of the cloud

whose angular momentum is between γ_* and γ_∞ . The first value depends on a characteristic radius for the magnetosphere (R_{mag}) of the star which estimates the inner edge of the disk. The magnetosphere truncates the disk at a radius (R_{mag}) around 10 stellar radii ($R_{\text{mag}} = 0.1 \text{ AU}$, Najita & Shu 1994; Shu et al. 1994), two orders of magnitude less than the value used in Nagel (2007a). The masses of the components depend on this value, but the mechanism for the distribution of the mass between the star, circumprimary and circumbinary disks do not depend on it. Taking the value used in Nagel (2007a), $\gamma_* = 0.432$ ($R_{\text{mag}} = 0.1 R_d$) and assuming that the disk and star form coevally, the mass of the star reaches a value of $M_* = 0.246$, and the disk accumulates more than three times this value, $M_d = 0.754$. These masses are given in units of the total mass that has fallen from the cloud since the beginning of the collapse. A decrease in the value of R_{mag} will increase the disk mass at the expense of the star mass. The important thing to note is that this configuration is far from an equilibrium state. Thus, eventually a gravitational instability arises, whose effect is to transfer material from the disk to the star until $M_d \ll M_*$. This instability could work to regulate the mass of the disk (Shu et al. 1993), a fact required from the observational point of view (Beckwith et al. 1990), where the last condition is always satisfied.

Another process that acts in the same sense comes from thermal instabilities, which are commonly used in the context of dwarf-nova systems (Lin, Papaloizou, & Faulkner 1985) and FU Orionis outbursts (Clarke, Lin, & Pringle 1990). These instabilities arise when the hydrogen ionization is not complete; in this case the opacity strongly depends on temperature and thermally-unstable regions are produced (Lin et al. 1985). The result is that at some time the mass accretion rate in the disk steeply increases, showing epochs of high luminosity, which can be sustained during $\sim 10^3 \text{ yr}$ after the outburst (see Clarke et al. 1990).

The conclusion is that the outcome of all the processes presented is the transfer of mass from the disk to the star, resulting in disks less massive than the star, consistent with observations.

4. ESTIMATION OF DISK MASSES USING THE JACOBI CONSTANT

4.1. Main ideas regarding the Jacobi constant

The main goal in this work is to use the formalism of the circular restricted 3-body problem, to obtain information about likely configurations for the binary system disks. First, we assume that the sys-

tem is well-represented by three bodies, thus, the evolution of the particle would only depend on the gravitational force exerted by the two stars. Moreover, if the orbit of the two stars is circular, then C_J is constant and can be written in the coordinate system rotating with the stars as:

$$C_J = x^2 + y^2 + 2\left(\frac{M_p}{r_p} + \frac{M_s}{r_s}\right) - v^2 \quad , \quad (3)$$

where the units of mass, time and distance are deduced by choosing $G = 1$, $M_\star = 1$, and the distance in units of the separation of the two stars. Here r_p and r_s are the distances to a particular point (x, y, z) from the primary and secondary stars, respectively and, finally, v is the magnitude of the velocity of the particle.

If the substitution $v^2 = 0$ is made, then an implicit relation is found, which represents, for a particle with an associated C_J , the locus of the so-called surface of zero-velocity. This surface is the boundary between zones where $v^2 < 0$, and $v^2 > 0$. The former is non-physical while the latter represents a possible physical state.

These restrictions are first studied for the case that the mass of the secondary star (M_s) is zero; i.e., an isolated star. The formation of a disk in this case is studied by Nagel (2007a). That paper describes the evolution of a dense ring evolving towards a Keplerian radius as a constant angular momentum feature; the trajectory is always located in a permissible region. Regarding the $M_s \ll 1$ case, we hope to identify configurations that restrict a particle to a specific region in space. If the material is located inside the orbit of the secondary it belong to a circumprimary disk. If the material is outside the secondary's orbit it would correspond to a circumbinary disk.

As the first step, we substitute $v^2 = 0$ and $M_s = 0$ in equation (3), obtaining

$$C_J = R^2 + \frac{2}{\sqrt{R^2 + Z^2}} \quad . \quad (4)$$

This implicit relation gives the location of the zero-velocity surface for each value of C_J . This equation only depends on the cylindrical radius (R) and the coordinate perpendicular to the plane of the disk (Z). Thus, these surfaces have azimuthal symmetry, as expected.

The orbital plane is located at $Z = 0$. Figure 1 shows some of these surfaces projected onto the RZ plane for various values of C_J . The plots are presented for $Z \geq 0$ as the curves below the orbital plane are symmetric. A particle with $C_J = 2$ can

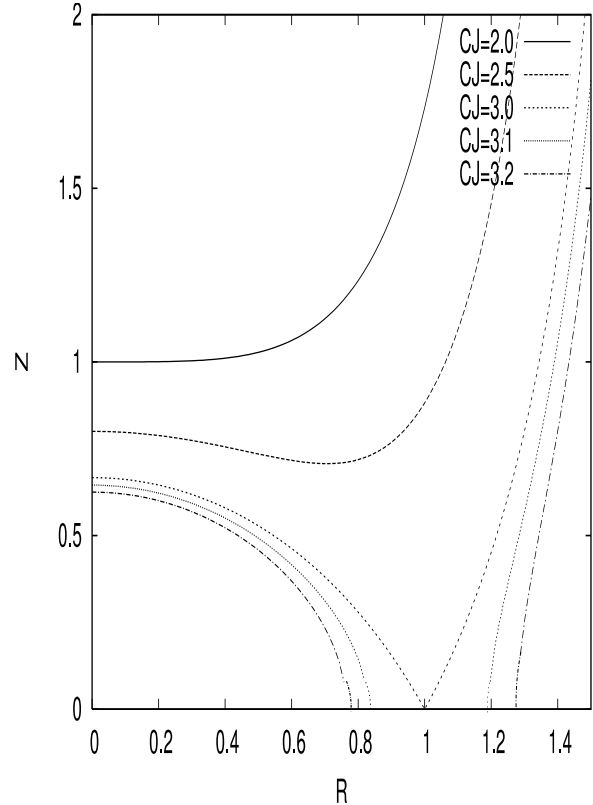


Fig. 1. Curves of zero-velocity in the RZ plane, for $C_J = 2$ (solid line), $C_J = 2.5$ (long-dashed line), $C_J = 3$ (short-dashed line), $C_J = 3.1$ (dotted line) and $C_J = 3.2$ (dot-dashed line) for the case $M_s = 0$.

only exist below the curve characterizing the particles's value for C_J . Because the whole orbital plane is an allowed region for this particle, its trajectory when falling from the cloud could reach the star. In other words, some of the cloud particles will end their evolution in the star. A $C_J = 3$ particle has an associated surface of zero-velocity touching the orbital plane, in this case at $R = 1$. For larger values of C_J , a couple of intersections are found in this plane ($Z1$ and $Z2$), which satisfy $Z1 > 1$ and $Z2 < 1$. In the orbital plane the allowed radii (R) are defined by the locus where $R > Z1$ and $R < Z2$. For $C_J < 3$ all the orbital plane is an allowed zone. Remember that for this analysis, it is first required to choose a specific particle, second, to calculate its C_J , and finally to search for the corresponding curve in Figure 1.

Even in the case of one star, for particles with $C_J \geq 3$ there is an inner and an outer permitted region. This configuration resembles a binary system with a circumprimary and circumbinary disk; note that in this case ($M_s = 0$) there is no circum-

secondary disk. Such a model is used in Mathieu (1994) and Mathieu et al. (1991, 1995) to describe the spectral energy distributions (SEDs) of spectroscopic binaries such as GW Orionis. A gap between these two regions represents the space cleared by the binary, phenomenon studied numerically and analytically in Artymowicz & Lubow (1994).

However, in practice the particles falling from the cloud will have a range in C_J . Thus, some of the particles are able to populate this space cleared by the binary. In the end we arrive at a continuous configuration of matter; its details depend on the particular initial configuration (see § 4.2).

From equation (4) and $Z = 0$, we obtain

$$R^3 - C_J R + 2 = 0 \quad , \quad (5)$$

a cubic equation that gives the location in the orbital plane of the zero-velocity surface for particles with given C_J .

Analytically, we can find the three solutions. As expected, none of the solutions is real positive for $C_J < 3$. For $C_J \geq 3$, there are two real positive solutions, that can be written as:

$$Z1 = 2(C_J/3)^{1/2} \cos \left[\frac{\arccos \left[- (3/C_J)^{3/2} \right]}{3} \right] \quad , \quad (6)$$

$$\begin{aligned} Z2 = & (C_J/3)^{1/2} \left[- \cos \left[\frac{\arccos \left[- (3/C_J)^{3/2} \right]}{3} \right] \right. \\ & \left. + 3^{1/2} \sin \left[\frac{\arccos \left[- (3/C_J)^{3/2} \right]}{3} \right] \right] \quad . \quad (7) \end{aligned}$$

The first one satisfies $Z1 \geq 1$ and the other $Z2 \leq 1$. The zone between these two radii is prohibited for material with Jacobi constant equal to C_J .

4.2. Application to a rigidly rotating cloud

All the ideas expressed in the last section can be applied to the collapse model developed in Ulrich (1976), where the cloud is rigidly rotating and the initial energy of the particles is zero. The expression for C_J using the inertial coordinate system is $C_J = 2(\Gamma_Z - E)$, where Γ_Z is the angular momentum perpendicular to the orbital plane, and E is the energy. The Jacobi constant of the falling particles in this case is given by:

$$C_J = 2 \left(\frac{R_d}{a} \right)^{1/2} \sin^2 \theta_o \quad , \quad (8)$$

where θ_o is the angle between the plane of the particle trajectory and the Z -axis.

The results of the last section require a specific value for R_d/a . In § 3.2, a first estimate gives $R_d/a \ll 1$, which is smaller than required for the formation of circumbinary disks. As stated in § 3.2, the processes needed for angular momentum transport are a key ingredient in raising the value for R_d/a , in order to end with a reasonable configuration. Magnetic braking could be extremely efficient for the transfer of angular momentum from the inner region of the collapsing cloud (Shu et al. 2006; Galli et al. 2006), in order to form a larger disk composed of an external shell in the rigidly-rotating cloud.

In the case $M_s = 0$, the distance a is meaningless, as there is no secondary star. Therefore, the evolution of a particle within the velocity field given by Ulrich (1976) is not subject to any restrictions due to a particular value for C_J . Thus, the analytic solution given in that paper is not changed. This conclusion does not mean that at some time certain particles will have $C_J > 3$. For such particles there exists a zero-velocity surface that restricts their trajectory to within an allowed zone.

4.3. Restrictions due to C_J in the $M_s = 0$ case

The next analysis treats the existence of zero-velocity curves for a particle moving in the orbital plane. The case $M_s = 0$ reduces to the problem of formation and evolution of a disk around an isolated star and is described in Nagel (2007a). The different stages outlined by Nagel (2007a) are further explored here. In the following, we treat the non-perturbed case for the problem with a small secondary star, as described in § 4.4.

4.3.1. Restrictions due to a shock in the orbital plane

The material falls to the orbital plane with a C_J given by equation (8); at its arrival there, a shock is produced. The shock involves the dissipation of the velocity perpendicular to this plane, which results in a variation of C_J , that can be written as:

$$C_J = 2 \left(\frac{a}{R_d} \right)^{1/2} R_I + \frac{\left[1 - \left(\frac{a}{R_d} \right) R_I \right]}{R_I} \quad . \quad (9)$$

In this relation R_I is the radius where a given particle intersects the orbital plane. The R and R^{-1} terms in equation (9) mean that C_J increases either at large R or small R . This feature permits us to find two solutions, $R_{I\pm}$, where $C_J = 3$; they are expressed as:

$$R_{I\pm} = \frac{(3+y) \pm \sqrt{(3+y)^2 - 8y^{1/2}}}{4y^{1/2}} \quad , \quad (10)$$

where $y = a/R_d$.

Because the condition for circumbinary formation is $y^{-1} = R_d/a > 1$, the physical range of y is $0 < y < 1$. Thus, the range in R_{I-} is $[0.293, 0.347]$, expressing that without any further interactions, the material initially located at radii of less than 0.293 will be unable to reach positions larger than 1. For R_{I+} , the range is from 1.707 to infinity; thus, particles at initial positions larger than 1.707 cannot move to radii less than 1. Remember that for $C_J = 3$, the curve of zero velocity is located at $R = 1$. The relevant space is restricted to $R_{I+} < y^{-1} = R_d/a$; evaluating this expression using equation (10), we obtain $R_d/a \geq 9/4$. Those configurations satisfying this last inequality will always have external material with $C_J > 3$.

4.3.2. Motion towards minimum-radius curve

Nagel (2007a) provides a detailed analysis of the implications of the minimum-radius curve. Here, we only point out that it represents the minimum position for particles evolving from R_I , in the first stage of disk formation. At the beginning, the material settles in allowed regions, then the evolution will move them also to allowed zones ($v^2 > 0$). As a function of time, the regions modify their size or even disappear, depending on the particular value of C_J assigned to the particle studied. Nagel (2007a) also showed that the particles move all the way towards the minimum-radius curve without interactions between them. In this case, the C_J for each particle is conserved, and the zero-velocity curves do not change their position. An inner region of the disk is absorbed by the star; the inner material of the remaining disk will eventually arrive to its minimum radius and will then acquire a positive radial velocity. Further evolution is described in Nagel (2007a); the main feature is an inner dense ring moving outwards, stopping at a Keplerian position. Our purpose in the rest of this Section is the analysis of such a dense ring.

4.3.3. Dense ring formation

The time it takes for the ring to move to its equilibrium position (t_{eq}) is assumed to be much less than Δt . Thus, there are three clearly separated time-scales, related through $t_{eq} \ll \Delta t \ll t_{ff}$. This assumption means that the material falling from the cloud onto the orbital plane during time t_{eq} may be neglected; thus, we assume that the dense ring contains all the material deposited in the orbital plane during the time Δt , which was not accumulated in the star. At its equilibrium radius, the ring will accumulate a clearly-defined section of the falling cloud, continuously increasing its mass (see details in Nagel 2007a).

At this stage, the relevant feature is the inner ring, which, moving outwards, becomes denser as it captures material. Our next objective is to follow the ring's evolution of C_J . A model that resembles the behavior of the ring as it evolves is required, that is, a set of positions with appropriate velocity. Such a model allows us to calculate the C_J for different locations of the dense ring.

The model adopted is of a ring accumulating material with specific angular momentum (γ) at position $R_{min}(\gamma)$. The arguments in favor of this model are found in Nagel (2007a) (for more details see Nagel 2007b), using their $R\gamma$ plots. The radial velocity (v_{min}) required represents the velocity at which the falling material arrive to R_{min} . Besides, the use of this model guarantees that the material located at the minimum radii curve has zero radial velocity at the arrival of the dense ring; thus, the only relevant feature is the dense ring moving along this curve with $v = v_{min}$.

If we substitute the position (R_{min}) and velocity (v_{min}) into equation (3), we obtain:

$$C_J = \left(\frac{2}{R_{min}} - v_{min}^2 - \frac{\gamma_a^2}{R_{min}^2} \right) y + 2\gamma_a y^{-1/2} \quad , \quad (11)$$

where γ_a is the mean angular momentum of all the material that has been absorbed by the ring (an expression for γ_a is deduced in Nagel (2007b)). The value of γ_a depends on γ , and thus C_J depends on γ and y . If we change y , the size of the disk (R_d) will be modified, and different positions for the ring ($R/a = (R_{min}(\gamma)/R_d)y^{-1}$) are obtained, with new values for C_J .

In equation 11, we can fix γ to see the behaviour in terms of y . The relevant cases are obtained for y corresponding to $C_J \geq 3$. We look for configurations with restrictions given by the presence of zero-velocity curves in the orbital plane.

The model is useful while $\gamma < 1$; the final configuration has the ring at $R_{min}(\gamma = 1)$. At this stage, the ring contains material with some range in initial angular momentum; there are two cases worth noting: (1) $0.43 < \gamma < 1$, and (2) $\gamma = 1$. These cases are based on Nagel (2007a); in the first one the formation begins at $R = R_{min}(\gamma = 0.43) = 0.1R_d$ and ends with all the material in the dense ring. The last case represents a ring with $\gamma = 1$, resembling the material that is continually arriving to this position.

The restricted state ($C_J > 3$) in case (1) puts the ring at $R/a > 1.65$, and for the case (2) at $R/a > 1.45$. Both cases place the ring outside the curves of zero-velocity, thus, the ring in principle can move to any larger radius, but inwards evolution will be

limited to the position of that curve. However, such a conclusion can only be reached by assuming that at later times the ring does not interact.

The process described by equation (11) can be seen in another way: given a value for y , an increase in γ means that the ring is moving outwards. Making the choice $y = 0.25$ as typical, and $\gamma_{\min} = 0.43$ (the specific angular momentum of the innermost ring that is not absorbed by the star), then C_J is a monotonic increasing function of γ , beginning with $C_J = 1.95$ ($\gamma = 0.43$) and ending with $C_J = 3.28$ ($\gamma = 0.99$). Arriving at $R = R_{\min}(\gamma = 0.87)$ the ring acquires $C_J = 3$, therefore, the position of the dense ring with associated curves of zero-velocity satisfies the inequality

$$R/a > \frac{R_{\min}(\gamma = 0.87)}{R_d} y^{-1} = 1.56 \quad . \quad (12)$$

These results allow us to conclude that the ring moves through $R/a = 1$ with $C_J < 3$. Thus, when it finally acquires $C_J = 3$, it lies in the outer allowed zone, such that the zero-velocity curves are on the inner side.

The radius $R/R_d = 1$ corresponds to the largest Keplerian radius. The final configuration is a dense ring that lies at a radius of less than one with null radial velocity.

The characteristic state for the ring is given for the case where the particles with the maximum value for γ are taken in the dense ring ($\gamma = 1$), and a radial velocity $v_R = 0$. This state for the ring used in equation (11) gives

$$C_J = \left(\frac{2}{R} - \frac{1}{R^2} \right) y + 2y^{-1/2} \quad , \quad (13)$$

which is the Jacobi constant for a particle with $v(R/R_d) = 0$ at the position R/R_d .

Figure 2 shows plots of C_J vs R/R_d for various values of y . The maximum of C_J occurs at $R/R_d = 1$ for every parameter y , and thus the most restricted configuration (where the external zero-velocity surface is at the largest radius for that y) occurs when the dense ring stops at the edge of the disk. The position of the secondary in units of R_d is $y = a/R_d$. The plots for $y < 0.5$ show that the ring stops outside the secondary orbit. For $y = 1$ the ring will stop inside this orbit. However, in this case there are no restrictions because $C_J < 3$. Anyhow, this is the extreme case that is considered here, where particles falling with the Ulrich (1976) solution represent the worst approximation. Thus, we argue that the dense ring becomes part of the circumbinary material with a strong annular feature, consistent with observations

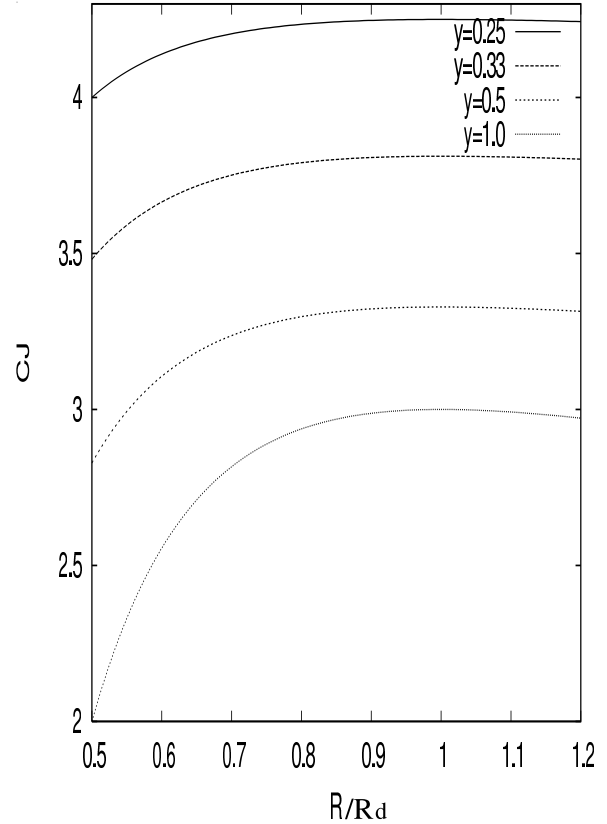


Fig. 2. Plots of C_J vs R/R_d , for a particle with $\gamma = 1$, and $v_R = 0$. The different curves correspond to $y = a/R_d = 0.25$ (solid line), $y = 0.33$ (long-dashed line), $y = 0.5$ (short-dashed line), and $y = 1$ (dotted line).

of GG Tau (Guilloteau et al. 1999), and UY Aur (Close et al. 1998). Note that the dense ring could have inner prohibited regions. However, this does not mean that the material falling from the cloud cannot incorporate into this zone.

Proceeding with this analysis, plots can be made of the positions ($Z1/R_d$) of the zero-velocity curves vs y for different R_* (here R_* represents the location where $v_R = 0$). The procedure is to substitute equation (13) into equation (6), and take $R = R_*$, thus obtaining a relation that depends on R_* and y . The first conclusion that can be extracted is that $R_* \geq Z1/R_d$, which is clearly expected. Figure 3 shows plots for $R_* = (0.6, 0.7, 0.8, 0.9, 1.0)$ and we note that the range of y plotted corresponds to $C_J \geq 3$, which can be expressed as $[0, y_*]$, where y_* depends on R_* .

Looking again at Figure 3, we see that there is some y (y_o) where the ring is located on the zero-velocity curve. It is interesting to note that y_o is close to y_* , and both coincide for the case $R_* = 1$.

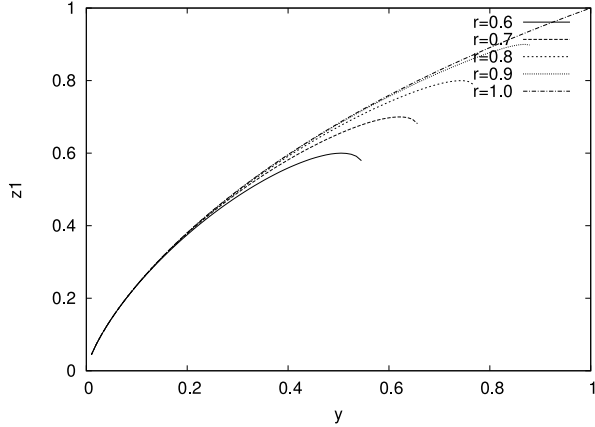


Fig. 3. Plots of $Z1/R_d$ vs y , for various radii. $R_* = 0.6$ (solid line), $R_* = 0.7$ (long-dashed line), $R_* = 0.8$ (short-dashed line), $R_* = 0.9$ (dotted line) and $R_* = 1.0$ (dot-dashed line). R_* represents the position where the dense ring stops.

It should be remembered (see § 3.2) that angular momentum transport processes are required to obtain reasonable values for the parameter y ; therefore by increasing the importance of such processes we will eventually get values of less than 1, but not too close to zero. Following this line of thought, values close to y_* are the best choices regarding the physical arguments just expressed, because a small variation in the state of the ring (or a section of it) can put it in the inner allowed zone; in other words, moving the particles to the circumprimary disk, instead of leaving them associated to the circumbinary disk. In this way, the ring could be divided between both disks (see § 5).

These results suggest that in a real situation the zero-velocity curve is near the ring. If at this stage the ring is free to move, then the likely evolution is an outward motion, allowing only small inward displacements. For the case $R_* = 1$ and the parameter $y = y_* = 1$, the dense ring lies on the zero-velocity curve. In this case inward motion is forbidden — an expected conclusion for particles moving in a Keplerian orbit, again assuming a non-interacting scheme.

All these ideas are extracted from the study of the $M_s = 0$ case. Our aim in this section is to describe the previously known evolution (Nagel 2007a) from the viewpoint of the conservation of C_J . In the next section we will examine the $M_s \ll 1$ case.

4.4. Restrictions due to C_J in the $M_s \ll 1$ case

The analysis developed in this paper is a qualitative one. Such information is extracted from a

conservation argument using the variable that is conserved. Thus, the next step required to address the $M_s \ll 1$ case is to argue that the presence of a secondary star will slightly disturb the trajectory and velocity of a particle found for the $M_s = 0$ case. From this point of view, the material in the orbital plane will move away from the one-star solution (see Nagel 2007a). Therefore, we look for configurations where a section of the disk is restricted ($C_J > 3$) to lie inside the secondary orbit (in a circumprimary disk), or outside of this orbit (as circumbinary material).

Here, we make the assumption that the material arrives at the orbital plane with the Ulrich (1976) solution and moves towards the minimum radius curve without interactions. For material moving near the secondary star, the interaction will appreciably modify the trajectories and velocities. However, for most of the matter the evolution towards the minimum radius curve is the same as for the $M_s = 0$ case. The simulations of the next section clarify this point.

Equation (11) gives us the C_J of the dense ring for a model representing the non-perturbed case (see § 4.3.3). There are two variables in equation (11), v_{\min} and R_{\min} , that can be adjusted to produce variations of this model. The variables that characterize the perturbed case are now called v_R and R .

Thus, the study of the function $f(R)$, given by,

$$f(R) = \frac{2}{R} - \frac{\gamma_a^2}{R^2}, \quad (14)$$

which contains all the R dependence, should tell us quantitatively the changes in C_J in terms of the position where the dense ring accumulates material of initial specific angular momentum γ . R must satisfy $R > R_{\min}(\gamma)$. Remember that γ_a depends on γ_{\min} , the minimum specific angular momentum that absorbs the dense ring.

Figure 4 shows $f(R)$ for various ranges of the specific angular momentum of the material contained in the dense ring. The first plot shown in Figure 4 covers the range $[0.43, 0.75]$ and it shows that $f(R)$ increases from $R_{\min}(0.75) = 0.297$ to 0.363 . This case represents the ring arriving at an intermediate stage. Another case, also presented in Figure 4, corresponds to the range $[0.43, 1.0]$. For this range, also, $f(R)$ increases, from $R_{\min}(1) = 0.5$ to 0.657 . The ranges in position where $f(R)$ rises are large enough to include with a high probability the configuration that occurs in the real case: where a secondary star disturbs the trajectory of the dense ring. This suggests that the trend for C_J in the $M_s \ll 1$ case is to grow, thus it is likely to find restrictions ($C_J > 3$) earlier

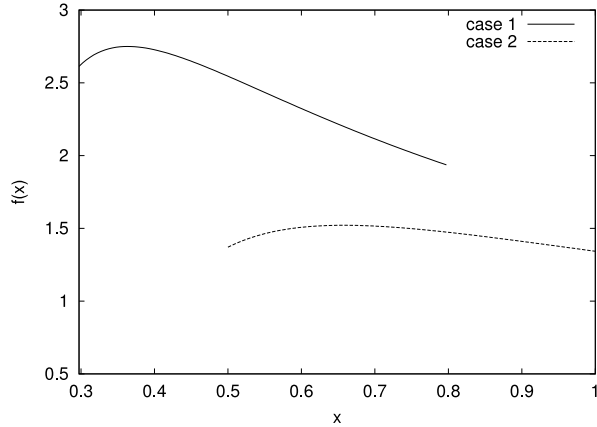


Fig. 4. Plots of $f(x, \gamma_a)$ vs x (see text for definition of $f(x, \gamma_a)$), where γ_a is the specific angular momentum of the dense ring. Two cases are analyzed, according to the angular momentum range of the material that the dense ring has absorbed. These are (1) $\gamma = [0.43, 0.75]$ (solid line), (2) $\gamma = [0.43, 1.0]$ (dashed line). The ranges in x are: 1) $R_{\min}(0.75) = 0.297$ to 0.8 , 2) $R_{\min} = 0.5$ to 1 .

than those in the $M_s = 0$ case. Variations in v_R are neglected, thus, $v_R = v_{\min}$ is given as typical in the case $M_s \ll 1$. Remember that $v_{\min} = dR_{\min}/dt_{\min}$, where $t_{\min} = t_{\gamma}^{R_{\min}(\gamma)}$, and R_{\min} and t are given in Nagel (2007a).

As noted, in equation (11) the change $R_{\min} \rightarrow R$, gives a relation for C_J in terms of γ , y and R . We explore this relation giving particular values to γ and R to find the value y where $C_J = 3$. We call this value y_{\min} , because for $y > y_{\min}$, $C_J > 3$. Table 1 contains the solution for some cases.

As noted in the last paragraph in § 4.3, the likely values for y in a real case are the values not close to zero, because $y^{-1} = R_d/a \gg 1$ requires an extremely efficient angular momentum transport mechanism. Besides, y too near one is not the best choice, because the assumption of material falling with the Ulrich (1976) solution cannot be used.

The four cases shown in Table 1, $\gamma = (0.43, 0.5, 0.6, 0.7)$, have the corresponding $v_{\min} = (-0.641, -0.685, -0.753, -0.827)$ and $R_{\min}/R_d = (0.1, 0.134, 0.192, 0.259)$. Remember that $R_{\text{ring}} \geq R_{\min}$. The cases in Table 1 that better fit the restrictions stated above are the ones with $\gamma = 0.43$ and $\gamma = 0.5$; the relevant range in y is $[0.274, 0.564]$ for the former and $[0.341, 0.543]$ for the latter. Different values for y in these ranges correspond to different positions R ; this value indicates the location of the ring where it is accumulating particles with angular momentum γ . A particular configuration is given by

TABLE 1

CONFIGURATIONS WITH $C_J > 3$ FOR THE OUTER DENSE RING

γ	R_{ring}/a	R_{ring}/R_d	$y_{\min} (C_J = 3)$
0.43	0.213	0.12	0.564
	0.547	0.16	0.293
	0.728	0.2	0.274
0.5	0.276	0.15	0.543
	0.532	0.19	0.357
	0.675	0.23	0.341
0.6	0.322	0.2	0.622
	0.489	0.24	0.491
	0.588	0.28	0.476
0.7	0.355	0.27	0.761
	0.449	0.31	0.690
	0.507	0.35	0.690

The first column gives the specific angular momentum (γ) of the last material absorbed by the dense ring. In the second one are given, for every γ , likely positions for the ring (R_{ring}/a). The third column gives R_{ring}/R_d . The fourth column lists y_{\min} , where $C_J = 3$. See definition in text.

a radius R_{ring}/R_d , thus, y_{\min} is the smallest value for such ring to have $C_J \geq 3$.

Another condition that should be fulfilled is $R_{\text{ring}}/a < 1$, in order to give likely configurations leading to a circumprimary disk. Remember that such restricted configurations could occur at one time but further evolution may not lead to a zero-velocity curve, such that the ring is able to move to any space configuration.

All this suggests that the circumprimary disk is composed of particles with initial angular momentum that ranges from $\gamma = 0.43$ to $\gamma = 0.5$. The rest of the disk material, with γ ranging from 0.5 to 1.0, will form a circumbinary disk. This configuration is consistent with the case that the dense ring begins to form and then stops absorbing material when $\gamma = 0.5$. In such a case, the ring evolves as circumprimary material. The ring that begins its formation with the material with $\gamma = 0.5$ follows the evolution for a dense ring (Nagel 2007a), arriving at an equilibrium configuration in a circumbinary orbit. In the following section, a set of simulations will shed light on this issue.

5. SIMULATIONS

In this section, we prove with the help of some simulations that the comment stressed at the end of the last section is credible in a real situation. The system chosen is a $1 M_{\odot}$ primary star with a $0.01 M_{\odot}$ secondary. A set of simulations is made for $y = a/R_d = (0.3, 0.4, 0.5, 0.6, 0.7)$. The *ansatz* chosen to prove is that the larger the value of y , the higher the probability to create a binary system with a circumprimary disk.

As an example, the value $y = 0.4$ can only create a restricted configuration ($C_J > 3$) if the ring has absorbed material with at most $\gamma = 0.5$. A dense ring, which contains material that originally had $\gamma > 0.5$, would require a larger y value to be restricted. Thus, for a larger value of y , there is the chance to end up with a more massive circumprimary disk, compared with the circumbinary one. Hence, the expected tendency to prove using this set of simulations is a positive correlation between circumprimary disk mass and y .

These simulations are developed using a Smooth Particle Hydrodynamics code, described in Monaghan (1992). In this method the system is described as a set of particles that are followed individually (in a Lagrangian frame), which can interact with their neighbours. Pressure and viscosity terms are included, and their contribution strongly depends on the characteristics of the particles close to the position of interest. The simulations use the isothermal equation of state $P = \rho c_s^2$, where c_s is the sound speed with $T = 10$ K as a typical temperature. A detailed temperature profile is not taken into account, because only the gravitational interaction is relevant in this study. The initial temperature gives a sound velocity lower than typical velocities; thus, in the first stage of the evolution, pressure and viscosity effects are not important; moreover, a specific value of the temperature is meaningless. At this stage the SPH code can be seen as a N-body code; afterwards, however, the strong hydrodynamical interactions dominate the evolution. Thus, changes in the temperature vary the quantitative but not the qualitative picture.

The physical space is restricted to the orbital plane and the initial surface density (Σ) is given by,

$$\Sigma = \frac{\dot{M}\Delta t}{4\pi R(1-R)^{1/2}} \quad , \quad (15)$$

where \dot{M} is the rate of mass accretion from the cloud into the star-disk system and R is given in units of R_d . This expression is calculated by means of the mass deposited in the orbital plane at each radius.

The mass of the particles that initially lie at $R < R_d$ is m_i ; the value depends on the simulation. This set of particles is surrounded by more massive particles (10 times m_i), that spread to a radius (6, 5, 4, 3.5, 3) times the separation of the stars. The total number of particles is (7727, 8559, 8559, 8975, 8975) for the cases $y = (0.3, 0.4, 0.5, 0.6, 0.7)$. The mass accretion rate from the cloud is $\dot{M} = 10^{-6} M_{\odot} \text{yr}^{-1}$. The initial inner side of the disk is located at $R/R_d = 0.43$ ($\gamma/\gamma_{\infty} = 0.43$); thus, the minimum radius for this ring is $0.1R_d$. The distance between the stars is always 40 AU and the size of the stars is 4 AU, which numerically means that the material inside this radius disappears from the simulation.

First, we give a general description that applies to all of the simulations. Initially, all the material in the orbital plane will move towards the star; eventually the inner edge of the ring will arrive at the secondary orbit. The side of the ring closer to the star is disturbed; thus, the azimuthal symmetry of the ring is lost. This does not impede the rest of the ring in its evolution towards its minimum radius. A dense ring forms (Nagel 2007a) and with its outward motion passes through $R/a = 1$, where the secondary star again disperses some of the material. A large amount of ring mass follows the behavior of the $M_s = 0$ case, with only minor disturbances. At the end, the qualitative picture that emerges resembles the basic characteristics of the formation of the dense ring in the $M_s = 0$ case. Thus, the conclusions obtained in § 4.3 can be used.

The problem is solved in an inertial frame. However, the plots in coordinate space are made by rotating the axes and all the velocities, so that the stars are always on the X-axis. A set of plots presented in Figures (5, 6, 7, and 8) show the main effects described above. A plot of the particle positions in the orbital plane is given in Figure 9 for the $y = 0.3$ case at time 0.45. At such a low value of $y = 0.3$ the inner ring disconnects itself from the dense ring, eventually arriving at the configuration shown in Figure 9 where it is clearly associated with orbits around the primary. For the case $y = 0.4$ (Figure 10), a ring of material also detaches itself from the dense ring, but earlier on; a detachment always occurs when we increase y . An outward ring of material unsuccessfully disconnects from the dense ring. The next simulation ($y = 0.5$, Figure 11) is qualitatively similar to the previous ones, in that the inner ring evolves inside the secondary orbit and becomes part of the proto-circumprimary disk.

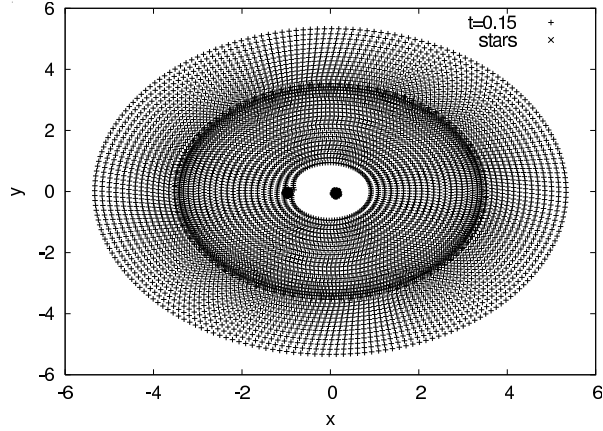


Fig. 5. A typical space configuration, at the arrival time of the inner ring to the secondary orbit. The time is $t = 0.15$ and the secondary star mass is $m = 0.1$. The two full circles at the center of the figure represent the positions of the stars. Any symbol $+$ indicates the position of a particle in space.

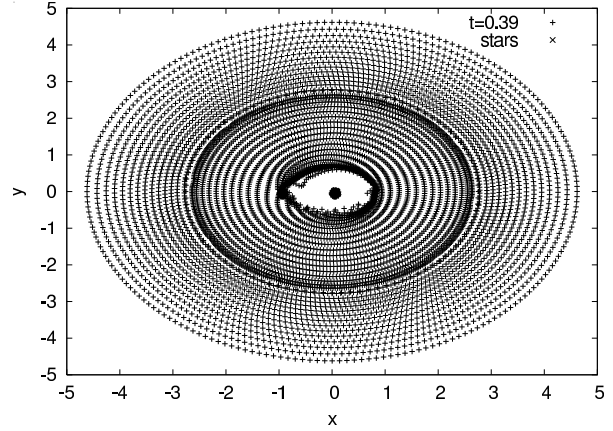


Fig. 7. The dense ring pass through the secondary orbit. The time is $t = 0.39$ and the secondary star mass is $m = 0.1$. The two full circles at the center of the figure represent the position of the stars. Any symbol $+$ indicates the position of a particle in space.

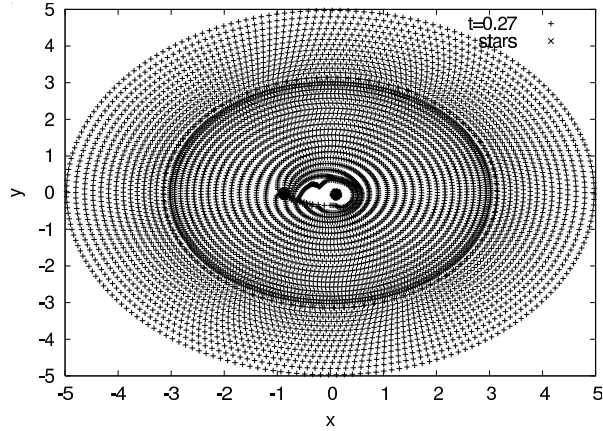


Fig. 6. Formation of a dense ring, in spite of the presence of the secondary star. The time is $t = 0.27$ and the secondary star mass is $m = 0.1$. The two full circles at the center of the figure represent the position of the stars. Any symbol $+$ indicates the position of a particle in space.

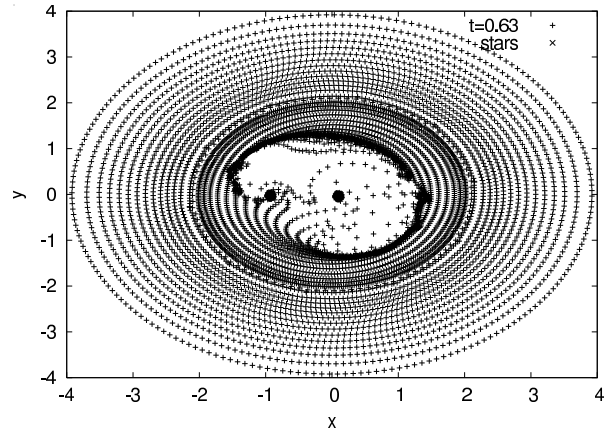


Fig. 8. An almost complete ring with outwards evolution. The time is $t = 0.63$ and the secondary star mass is $m = 0.1$. The two full circles at the center of the figure represent the position of the stars. Any symbol $+$ indicates the position of a particle in space.

The effect of increasing y up to $y = 0.6$ can be seen in Figure 12. There, another ring begins to detach itself from the dense ring. Thus, the material forming the circumprimary disk has an initial specific angular momentum ranging from 0.43 to 0.55. The result of the last simulation ($y = 0.7$, Figure 13) is analogous to the previous one. However, the range in γ of the material orbiting inside the radius $R/a = 1.0$ is larger, $0.43 < \gamma < 0.61$. In addition, the time when the inner ring is detached

decreases with increasing y . The simulation with $y = 0.5$ was repeated, increasing the spatial resolution by a factor of 4. A comparison of the simulation with both resolutions tells us that all the essential features are present despite the difference in resolution. Thus, the lower resolution simulation is adequate to extract the required information.

The range in γ assigned to the material in the circumprimary disk for the previous two cases allows us to estimate the mass associated with the disk. This

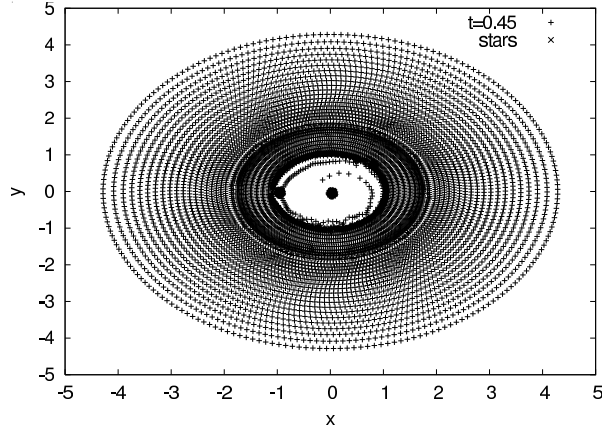


Fig. 9. Picture of the disk, for $y = 0.3$. An inner ring disconnects from the dense ring. The time is $t = 0.45$ and the secondary star mass is $m = 0.01$. The two full circles at the center of the figure represent the position of the stars. Any symbol $+$ indicates the position of a particle in space.

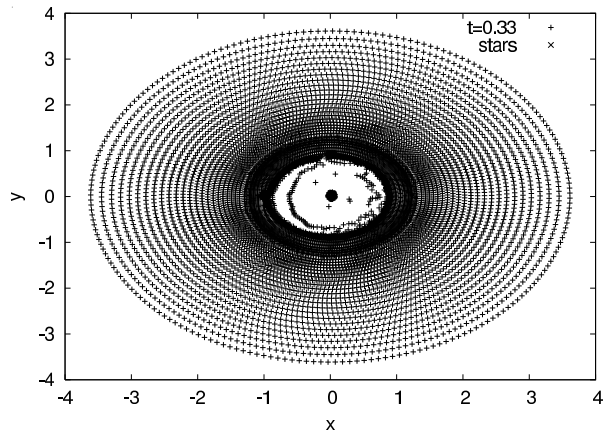


Fig. 10. Picture of the disk, for $y = 0.4$. The time is $t = 0.33$ and the secondary star mass is $m = 0.01$. The two full circles at the center of the figure represent the position of the stars. Any symbol $+$ indicates the position of a particle in space.

mass is calculated by noting that every particle in a shell of the cloud can be assigned a value of γ . Moreover, the solution of Ulrich (1976) gives the approximate position where every particle of the shell arrives to the orbital plane. Thus, the integral of the mass contribution of each particle allows us to describe the initial mass profile in the disk as:

$$M = \dot{M} \Delta t \left[- (1 - \gamma)^{1/2} \Big|_{\gamma_1}^{\gamma_2} \right], \quad (16)$$

where γ_1 and γ_2 define the range of angular momentum that is considered.

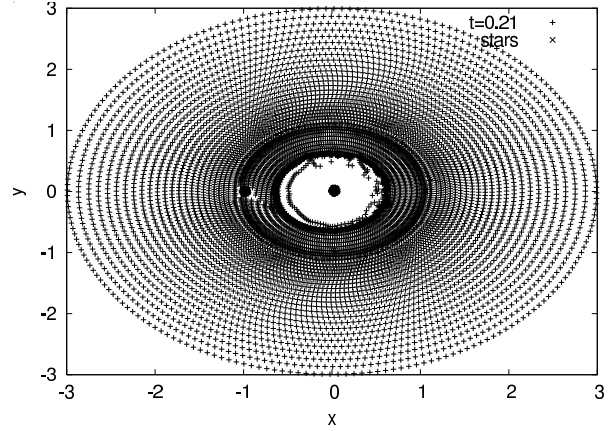


Fig. 11. Picture of the disk, for $y = 0.5$. The time is $t = 0.21$ and the secondary star mass is $m = 0.01$. The two full circles at the center of the figure represent the position of the stars. Any symbol $+$ indicates the position of a particle in space.

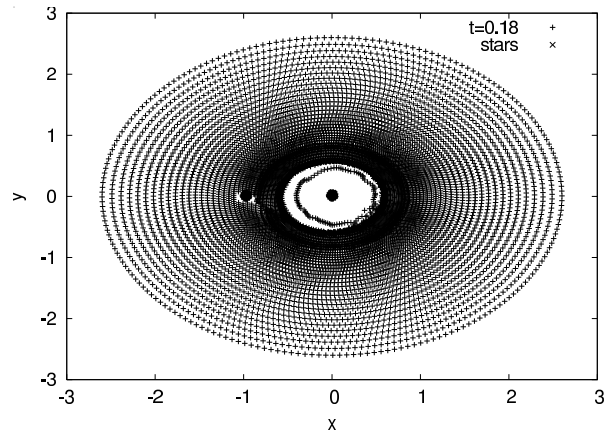


Fig. 12. Picture of the disk, for $y = 0.6$. The time is $t = 0.18$ and the secondary star mass is $m = 0.01$. The two full circles at the center of the figure represent the position of the stars. Any symbol $+$ indicates the position of a particle in space.

Using equation (16), the mass of the circumpriary disk (M_{cp}) for the case with $y = 0.6$ is 0.08; for the case with $y = 0.7$, the disk mass is 0.13. Naturally, it is possible to say that material with larger values of γ is associated with a circumbinary disk. Thus, in the first case, the circumbinary mass (M_{cb}) is 0.67; the second case has $M_{cb} = 0.63$. The sum of M_* , M_{cp} and M_{cb} is always one. The estimate of M_* is a lower limit for the final configuration because the material of the inner disk continually accretes towards the star. We assume that both disks evolve at the same rate; thus M_{cp} and M_{cb} are good estimates

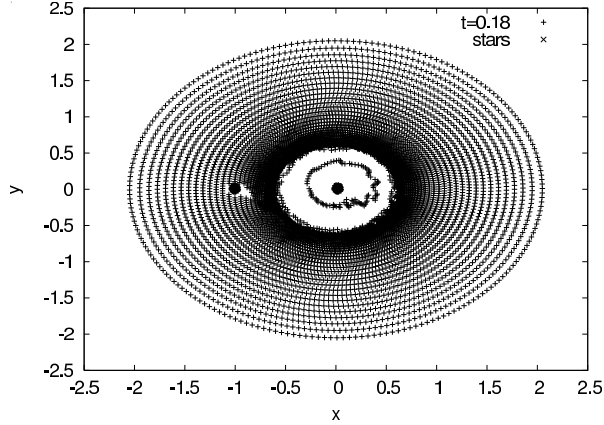


Fig. 13. Picture of the disk, for $y = 0.7$. The time is $t = 0.18$ and the secondary star mass is $m = 0.01$. The two full circles at the center of the figure represent the position of the stars. Any symbol + indicates the position of a particle in space.

of the disk masses. The ratio between M_{cp} and M_{cb} is 0.12 and 0.20, respectively, according to a typical binary stellar system. For example, in *UY Aur* (Duvert et al. 1998), $M_{cb} \approx 10^{-2}$ and $M_{cp} \approx 10^{-3}$, thus, $M_{cp}/M_{cb} \approx 0.1$.

The conclusion of these simulations is that the larger the value of y , the larger the amount of material that it is restricted to a circumprimary disk. Thus, an agreement is found between the conclusions of § 4 and the simulations described here.

6. CONCLUSIONS

Following the results of the simulation of the collapse of a rigidly rotating cloud to form a disk around an isolated star (Nagel 2007a), it is natural to separate all the falling material in two parts: one is directly incorporated into the star and the other into the disk. Neglecting the presence of angular momentum transport in the disk, this model is valid for massive disks, in which it is easy for instabilities to appear (Shu et al. 1993). The effect of these instabilities is to remove angular momentum from the disk, allowing some of the material to accrete to the star. One expects that the instabilities work faster when the disk is heavier; thus, most of the time the disk will have less mass than the star (M_*); see Shu et al. (1993). This leads to the conclusion that the mass of the disk(s) (M_d) is composed of a section of the cloud falling during a time Δt , which is smaller than the free-fall time (t_{ff}). Said another way, the consequence of the disparity in Δt and t_{ff} is that $M_d \ll M_*$.

An estimation of t_{ff} is obtained by assuming that $\dot{M}t_{ff} = M_*$. Here, M_* is the total stellar mass and \dot{M} is the mass accretion rate from the cloud. The latter is estimated using $\dot{M} = m_o c_s^3 / G$, which is taken from the collapse of an isothermal sphere (Shu 1977); $m_o = 0.975$ and c_s is the sound speed. For a $T = 10$ K cloud, \dot{M} equals $5.56 \times 10^{-6} M_\odot \text{ yr}^{-1}$.

The GW Ori primary star mass is about $2.5 M_\odot$, and the largest estimation for the secondary star mass is $1.3 M_\odot$ (Mathieu et al. 1995); thus, $t_{ff} = 6.83 \times 10^5 \text{ yr}$. An estimate for the circumbinary disk mass is $0.3 M_\odot$ (Mathieu et al. 1995); using this mass and the same value for \dot{M} , it is obtained $\Delta t = 5.39 \times 10^4 \text{ yr}$. For the binary system V4046 Sgr (Jensen & Mathieu 1997), the total stellar mass is $1.4657 M_\odot$; using the same value for \dot{M} , $t_{ff} = 2.63 \times 10^5 \text{ yr}$. The estimate of the circumbinary disk mass is $8.36 \times 10^{-3} M_\odot$; thus, $\Delta t = 1.50 \times 10^3 \text{ yr}$. Thus, $\Delta t \ll t_{ff}$, and the disk in both cases safely lies in a stable configuration, susceptible for the treatment described in this paper.

The binary system and any particle of the surrounding material is described as a three-body problem, in order to explore the consequences of the conservation of the Jacobi constant. Such a simplification does not mean that particle interactions are neglected. We can describe this situation in the context of the three-body problem as a particle continually changing its value of C_J , when the interactions are present. The consequence is that for every particle, the locations of its associated zero-velocity surfaces also change. Following these ideas, we describe the evolution of the material at the first stages of disk formation, in the $M_s = 0$ case, including the dense ring evolution with positive velocities, until it settles into a Keplerian orbit (Nagel 2007a). For the study of the dense ring we require a model that gives pairs of values for the position and velocity as a function of time. A reasonable configuration is one in which the ring evolves along the minimum radius curve (see § 4.3) with appropriate velocity.

Application of this model to the $M_s \ll 1$ case, lead to likely configurations which suggest the existence of material restricted to move inside the secondary-star orbit and some material that always moves outside of it. The former represents a circumprimary disk and the latter a circumbinary disk. A parameter that plays a role in this problem is the ratio between the separation of the stars (a) and the disk radius R_d (which is the largest possible Keplerian position), $y = a/R_d$, which is a measure of the importance of the angular momentum transport mechanisms at the binary system forma-

tion stage. Semi-analytic arguments (§ 4.4) and simulations (§ 5) lead to the conclusion that y values larger than 0 but not too close to 1 are the best choices for the formation of massive circumprimary disks. From these same simulations we conclude that the larger the value of y , the larger the mass of the circumprimary disk.

As an example, for $y = 0.6$, the estimation of the circumprimary disk mass (M_{cp}) is 0.08 times the mass that accretes from the cloud during the time Δt . The circumbinary disk mass (M_{cb}) is 0.67 times the same total accreted mass. A drawback of this result is that y is a parameter that is not directly found from observation. Thus, a comparison between simulations and observations is not obvious. The model of a disk with a gap that separates the circumprimary and circumbinary disk is used by Mathieu et al. (1995) to interpret the observed SED of GW Ori. The ratio between the disk masses (M_{cp}/M_{cb}) is equal to 0.13; this is almost the same value as that calculated in the model for $y = 0.6$, where $M_{cp}/M_{cb} = 0.12$. A conclusion that follows is that for GW Ori, $y = 0.6$, although this conclusion should be treated with caution, due to all the assumptions made in the observational interpretation (Mathieu 1994; Mathieu et al. 1991, 1995) and the assumptions made in this paper.

I thank Jorge Cantó for his continued support and advice. The assistance of William Lee in the numerical part of this research is gratefully acknowledged. I am in debt to the referee whose comments helped to clarify the subject of this paper. I also thank William Lee for a critical reading of the original version of the paper. The help of Stan Kurtz with the writing of the final version of the article is also acknowledged.

REFERENCES

- Artymowicz, P., & Lubow, S. H. 1994, *ApJ*, 421, 651
 Bate, M. R. 2000, *MNRAS*, 314, 33
 Beckwith, S. V. W., Sargent, A. I., Chini, R. S., & Guesten, R. 1990, *AJ*, 99, 924
 Bodenheimer, P., & Laughlin, G. 1995, *RevMexAA (SC)*, 1, 157
 Boss, A. P. 1998, *ApJ*, 503, 923
 Clarke, C. J., Lin, D. N. C., & Pringle, J. E. 1990, *MNRAS*, 242, 439
 Close, L. M., et al. 1998, *ApJ*, 499, 883
 D'Alessio, P., Calvet, N., & Hartmann, L. 1997, *ApJ*, 474, 397
 Duchene, G., Menard, F., Duvert, G., & Stapelfeldt, K. 2000, *BAAS*, 33, 717
 Dutrey, A., Guilloteau, S., & Simon, M. 1994, *A&A*, 286, 149
 Duvert, G., Dutrey, A., Guilloteau, S., Menard, F., Schuster, K., Prato, L., & Simon, M. 1998, *A&A*, 332, 867
 Galli, D., Lizano, S., Shu, F. H., & Allen, A. 2006, *ApJ*, 647, 374
 Guilloteau, S., Dutrey, A., & Simon, M. 1999, *A&A*, 348, 570
 Hartmann, L. W., & Kenyon, S. J. 1990, *ApJ*, 349, 190
 Hogerheijde, M. R., van Langevelde, H. J., Mundy, L. G., Blake, G. A., & van Dishoeck, E. F. 1997, *ApJ*, 490, L99
 Jensen, E. L. N., & Akeson, R. L. 2003, *ApJ*, 584, 875
 Jensen, E. L. N., Koerner, D. W., & Mathieu, R. D. 1996, *AJ*, 111, 2431
 Jensen, E. L. N., & Mathieu, R. D. 1997, *AJ*, 114, 301
 Jijina, J., Myers, P. C., & Adams, F. C. 1999, *ApJS*, 125, 161
 Lin, D. N. C., Papaloizou, J., & Faulkner, J. 1985, *MNRAS*, 212, 105
 Monaghan, J. J. 1992, *ARA&A*, 30, 543
 Mathieu, R. D. 1994, *ARA&A*, 32, 465
 Mathieu, R. D., Adams, F. C., Fuller, G. A., Jensen, E. L. N., Koerner, D. W., & Sargent, A. I. 1995, *AJ*, 109, 2655
 Mathieu, R. D., Adams, F. C., & Latham, D. W. 1991, *AJ*, 101, 2184
 Mouschovias, T. Ch., & Paleologou, E. V. 1979, *ApJ*, 230, 204
 Murray, C. D., & Dermott, S. F. 1999, *Solar System Dynamics* (Cambridge: Cambridge Univ. Press)
 Nagel, E. 2007a, *RevMexAA*, 43, 257
 Nagel, E. 2007b, Ph.D Thesis, Universidad Nacional Autónoma de México, Mexico
 Najita, J. R., & Shu, F. H. 1994, *ApJ*, 429, 808
 Nakamoto, T., & Nakagawa, Y. 1994, *ApJ*, 421, 640
 Osorio, M., D'Alessio, P., Muzerolle, J., Calvet, N., & Hartmann, L. 2003, *ApJ*, 586, 1148
 Shakura, N. I., & Sunyaev, R. 1973, *A&A*, 24, 337
 Shu, F. H. 1977, *ApJ*, 214, 488
 Shu, F. H., Galli, D., Lizano, S., & Cai, M. 2006, *ApJ*, 647, 382
 Shu, F. H., Najita, J., Galli, D., Ostriker, E., & Lizano, S. 1993, in *Protostars and Planets III*, ed. E. H. Levy & J. I. Lunine (Tucson: Univ. Arizona Press), 3
 Shu, F. H., Najita, J. R., Ostriker, E., Wilkin, F., Ruden, S., & Lizano, S. 1994, *ApJ*, 429, 781
 Smith, K. W., Bonnell, I. A., Emerson, J. P., & Jenness, T. 2000, *MNRAS*, 319, 991
 Stapelfeldt, K. R., Krist, J. E., Menard, F., Bouvier, J., Padgett, D. L., & Burrows, C. J. 1998, *ApJ*, 502, L65
 Szebehely, V. 1967, *Theory of Orbits: the Restricted Problem of Three Bodies* (New York: Academic Press)
 ————. 1980, *Celest. Mech.*, 22, 7
 Szebehely, V., & Mckenzie, R. 1981, *Celest. Mech.*, 23, 3

Ulrich, R. K. 1976, ApJ, 210, 377

Velusamy, T., Langer, W. D., & Goldsmith, P. F. 2002,
ApJ, 565, L43

Weintraub, D. A., Zuckerman, B., & Masson, C. R. 1989,
ApJ, 344, 915

Yorke, H. W., & Bodenheimer, P. 1999, ApJ, 525, 330